Preprint typeset in JHEP style - PAPER VERSION ZU-TH 04/09, IPPP/09/15

NNLO moments of event shapes in e^+e^- annihilation

arXiv:0903.4658v2 [hep-ph] 27 May 2009

A. Gehrmann–De Ridder

Institute for Theoretical Physics, ETH, CH-8093 Zürich, Switzerland
E-mail: gehra@phys.ethz.ch

T. Gehrmann

Institut für Theoretische Physik, Universität Zürich, Winterthurerstrasse 190, CH-8057 Zürich, Switzerland
E-mail: thomas.gehrmann@physik.unizh.ch

E.W.N. Glover

Institute for Particle Physics Phenomenology, Department of Physics, University of Durham, Durham, DH1 3LE, UK
E-mail: e.w.n.glover@durham.ac.uk

G. Heinrich

Institute for Particle Physics Phenomenology, Department of Physics, University of Durham, Durham, DH1 3LE, UK
E-mail: gudrun.heinrich@durham.ac.uk

Abstract: We compute the next-to-next-to-leading order (NNLO) QCD corrections to the first five moments of six event shape variables related to three-particle final states in electron-positron annihilation; the thrust, the heavy jet mass, the C-parameter, the wide and total jet broadenings and the three-to-two-jet transition parameter in the Durham algorithm Y_3. The NNLO corrections to the first moment are moderate for all event shapes, while the renormalisation scale dependence of the theoretical prediction is substantially reduced compared to the previously existing NLO results. From a comparison with data from JADE and OPAL, we observe that the energy dependence of the moments of the wide jet broadening and Y_3 can be largely explained without any non-perturbative power corrections, while the other observables exhibit a clear need for power-like contributions at low centre-of-mass energy.

Keywords: QCD, Jets, LEP and ILC Physics, NLO and NNLO Computations.

1. Introduction

Event shape variables in e^+e^- annihilation provide an ideal testing ground to study Quantum Chromodynamics (QCD) and have been measured and studied extensively in the last two decades. In particular, event shape variables are interesting for studying the interplay between perturbative and non-perturbative dynamics. Apart from distributions of these observables, to which the NNLO corrections recently have become available [1–6], one can also study mean values and higher moments. The nth moment of an event shape observable y is defined by

$$\langle y^n \rangle = \frac{1}{\sigma_{\mathrm{had}}} \int_0^{y_{\max}} y^n \frac{\mathrm{d}\sigma}{\mathrm{d}y} \mathrm{d}y \ , \tag{1.1}$$

where $y_{\max}$ is the kinematically allowed upper limit of the observable. Moments were measured for a variety of different event shape variables in the past. The most common observables y of three-jet type are: thrust T [7] (where moments of $y = (1-T)$ are taken), the heavy jet mass $\rho = M_H^2/s$ [8], the C-parameter [9], the wide and total jet broadenings B_W and B_T [10], and the three-to-two-jet transition parameter in the Durham algorithm Y_3 [11]. Definitions for all observables are given in, for example, Ref. [1]. Moments with $n \geq 1$ have been measured by several experiments, most extensively by JADE [12] and OPAL [13], but also by DELPHI [14] and L3 [15]. A combined analysis of JADE and OPAL results has been performed in Ref. [16].

As the calculation of moments involves an integration over the full phase space, they offer a way of comparing to data which is complementary to the use of distributions, where in general cuts on certain kinematic regions are applied. Furthermore, the two extreme kinematic limits – two-jet-like events and multi-jet-like events – enter with different weights in each moment: the higher the order n of the moment, the more it becomes sensitive to the multi-jet region. Therefore it is particularly interesting to study the NNLO corrections to higher moments of event shapes, as these corrections should offer a better description of the multi-jet region due to the inclusion of additional radiation at parton level.

Moments of event shape variables can be divided into a perturbative and a non-perturbative part,

$$\langle y^n \rangle = \langle y^n \rangle_{\mathrm{pt}} + \langle y^n \rangle_{\mathrm{np}} \ , \tag{1.2}$$

where the non-perturbative part accounts for hadronisation effects. The non-perturbative part is suppressed by powers of λ_p/Q^p ($p \geq 1$), where $Q \equiv \sqrt{s}$ is the centre of mass energy and λ_1 is of the order of Λ_{QCD}. The functional form of λ_p has been discussed quite extensively in the literature, but as this parameter is closely linked to non-perturbative effects, it cannot be fully derived from first principles.

The power corrections can be related to infrared renormalons in the perturbative QCD expansion for the event shape variable [17–24]. The analysis of infrared renormalon ambiguities suggests power corrections of the form λ_p/Q^p, but cannot make unique predictions for λ_p: it is only the sum of perturbative and non-perturbative contributions in (1.2) that becomes well-defined [25]. Different ways to regularize the IR renormalon singularities have been worked out in the literature. One approach is to introduce an IR cutoff μ_I and to

replace the strong coupling constant below the scale μ_I by an effective coupling such that the integral of the coupling below μ_I has a finite value [23, 24]

$$\frac{1}{\mu_I}\int_0^{\mu_I} dQ\,\alpha_{\rm eff}(Q^2) = \alpha_0(\mu_I)\;. \tag{1.3}$$

This dispersive model for the strong coupling leads to a shift in the distributions

$$\frac{\mathrm{d}\sigma}{\mathrm{d}y} = \frac{\mathrm{d}\sigma_{\rm pt}}{\mathrm{d}y}\,(y - a_y\,\mathcal{P})\;, \tag{1.4}$$

where the numerical factor a_y depends on the event shape, while $\mathcal{P}$ is believed to be universal and scales with the CMS energy like μ_I/Q. We refer the interested reader to Refs. [24, 26, 27] for further details.

Another ansatz is that of Korchemsky et al. [28,29] who suggest a shape function valid equally for thrust, C-parameter and heavy jet mass ρ, which is independent of the energy scale and takes into account the energy flow into two hemispheres of the final state. In the region $y \gg \Lambda_{QCD}/Q$, their predictions for the mean values of $1-T$ and ρ coincide with those of renormalon based models, i.e. the leading power corrections are parametrised by a single non-perturbative scale λ_1. In the case of the C-parameter however, they find an additional contribution modifying the size of the $1/Q$ correction. This formalism also allows one to study the region $y \sim \Lambda_{QCD}/Q$, where power corrections of the form $(\Lambda_{QCD}/(Qy))^p$ for arbitrary p become important.

Gardi et al. [30–33] make an analysis using the formalism of the so-called "dressed gluon exponentiation" [32], which resums the renormalon contribution to the Sudakov exponent, taking into account factorially enhanced subleading logarithms. Within this formalism, power law corrections beyond the leading term are predicted which probe the region $y \sim \Lambda_{QCD}/Q$. In particular, this formalism predicts that power corrections of the form λ_2/Q^2 are suppressed, which is also indicated by the data. Ref. [33] contains a detailed analysis of the power corrections for the thrust and heavy jet mass distributions, taking also hadron mass effects into account and deducing from renormalon analysis that the non-perturbative corrections to both distributions can be described by a single shape function. In Ref. [31], characteristic functions describing the leading and subleading power corrections to the first four moments of the thrust variable are derived.

In Ref. [34], a renormalisation group improved (RGI) treatment of the first moment of event shape observables is suggested and compared to data. A simultaneous fit of three parameters – Λ_{QCD}, a parameter ρ_2 describing uncalculated perturbative higher order corrections and a parameter K_0 controlling the power corrections – showed for the cases of $\langle 1-T\rangle$ and $\langle\rho\rangle$ that the data are consistent with $K_0 = 0$ within the RGI approach without leading to unreasonably large values of ρ_2, but do not allow definite conclusions.

Overviews on the various approaches to estimate non-perturbative corrections can be found in Refs. [25,35]. Recently, significant progress in the theoretical description of power corrections has also been made using Soft-Collinear Effetive Theory (SCET [36–38]), see e.g. Ref. [39].

An extensive comparison of e^+e^- data on events shapes with NLO+NLLA QCD predictions, supplemented by power corrections within the approach of [23, 24], has been

performed in [40]. A determination of α_s and α_0 from fits to distributions and mean values of five event shapes has been carried out, and indications were found that uncalculated higher orders may contribute significantly to the non-perturbative corrections. A determination of α_s based on moments of event shapes calculated up to NLO has recently been reported in [41].

Based on the NNLO corrections published in [1], several new determinations of the strong coupling constant have become available recently. In Ref. [42], fits of six event shape distributions to ALEPH data have been made. In [43], the same perturbative results have been fitted to JADE data, including also matching [44] onto the resummation of large logarithms [45] in the next-to-leading log approximation (NLLA).

A very recent study of non-perturbative contributions to the thrust distribution, based on the NNLO corrections published in [1] and including NLLA resummation, as well as power corrections within the low-scale effective coupling formalism [23, 24], can be found in [46]. This work also provides a determination of α_s and α_0 based on fits to a wealth of experimental data for the thrust distribution and confirms the conjecture of [40] that the explicit $1/Q$ corrections become smaller as higher perturbative orders are included. This corroborates the hypothesis that the divergent renormalon contribution can be regularized by modifying the strong coupling at low scales, leading to the effective coupling used in eq. (1.3).

In this paper, we provide the NNLO corrections to the first five moments of the event shapes thrust T, the normalised heavy jet mass ρ, the C-parameter, the wide and total jet broadenings B_W and B_T and the transition from three-jet to two-jet final states in the Durham jet algorithm Y_3. After reviewing the theoretical framework and fixing the notation in Section 2, we present results for the NNLO coefficients of the first five moments of the above-mentioned event shape distributions in Section 3. The numerical impact of these corrections and implications for the description of experimental event shape data are discussed in Section 4.

2. Theoretical framework

The perturbative expansion for the distribution of a generic event shape observable y up to NNLO at centre-of-mass energy $\sqrt{s}$ for renormalisation scale $\mu^2 = s$ and $\alpha_s \equiv \alpha_s(s)$ is given by

$$\frac{1}{\sigma_{\rm had}}\frac{\mathrm{d}\sigma}{\mathrm{d}y} = \left(\frac{\alpha_s}{2\pi}\right)\frac{\mathrm{d}\bar{A}}{\mathrm{d}y} + \left(\frac{\alpha_s}{2\pi}\right)^2\frac{\mathrm{d}\bar{B}}{\mathrm{d}y} + \left(\frac{\alpha_s}{2\pi}\right)^3\frac{\mathrm{d}\bar{C}}{\mathrm{d}y} + \mathcal{O}(\alpha_s^4)\,. \tag{2.1}$$

Here the event shape distribution is normalised to the total hadronic cross section $\sigma_{\rm had}$. With the assumption of massless quarks, then at NNLO we have,

$$\sigma_{\rm had} = \sigma_0\left(1 + \frac{3}{2}C_F\left(\frac{\alpha_s}{2\pi}\right) + K_2\left(\frac{\alpha_s}{2\pi}\right)^2 + \mathcal{O}(\alpha_s^3)\right)\,, \tag{2.2}$$

where the Born cross section for $e^+e^- \to q\bar{q}$ is

$$\sigma_0 = \frac{4\pi\alpha}{3s}N\,e_q^2\,. \tag{2.3}$$

The constant K_2 is given by [47–49]

$$K_2 = \frac{1}{4}\left[-\frac{3}{2}C_F^2 + C_F C_A\left(\frac{123}{2} - 44\zeta_3\right) + C_F T_R N_F\left(-22 + 16\zeta_3\right)\right], \tag{2.4}$$

where the QCD colour factors are

$$C_A = N, \qquad C_F = \frac{N^2-1}{2N}, \qquad T_R = \frac{1}{2} \tag{2.5}$$

for $N = 3$ colours and N_F light quark flavours.

The perturbative QCD expansion of $\langle y^n \rangle$ is then given by

$$\langle y^n \rangle(s, \mu^2 = s) = \left(\frac{\alpha_s}{2\pi}\right)\bar{\mathcal{A}}_{y,n} + \left(\frac{\alpha_s}{2\pi}\right)^2 \bar{\mathcal{B}}_{y,n} + \left(\frac{\alpha_s}{2\pi}\right)^3 \bar{\mathcal{C}}_{y,n} + \mathcal{O}(\alpha_s)^4 . \tag{2.6}$$

In practice, we compute the perturbative coefficients $\mathcal{A}_n$, $\mathcal{B}_n$ and $\mathcal{C}_n$, which are all normalised to σ_0:

$$\frac{1}{\sigma_0}\int_0^{y_{\max}} \mathrm{d}y\, y^n \frac{\mathrm{d}\sigma}{dy} = \left(\frac{\alpha_s}{2\pi}\right)\mathcal{A}_{y,n} + \left(\frac{\alpha_s}{2\pi}\right)^2 \mathcal{B}_{y,n} + \left(\frac{\alpha_s}{2\pi}\right)^3 \mathcal{C}_{y,n} + \mathcal{O}(\alpha_s^4) . \tag{2.7}$$

$\mathcal{A}_{y,n}$, $\mathcal{B}_{y,n}$ and $\mathcal{C}_{y,n}$ are straightforwardly related to $\bar{\mathcal{A}}_{y,n}$, $\bar{\mathcal{B}}_{y,n}$ and $\bar{\mathcal{C}}_{y,n}$ by

$$\begin{aligned}
\bar{\mathcal{A}}_{y,n} &= \mathcal{A}_{y,n} , \\
\bar{\mathcal{B}}_{y,n} &= \mathcal{B}_{y,n} - \frac{3}{2}C_F\,\mathcal{A}_{y,n} , \\
\bar{\mathcal{C}}_{y,n} &= \mathcal{C}_{y,n} - \frac{3}{2}C_F\,\mathcal{B}_{y,n} + \left(\frac{9}{4}C_F^2 - K_2\right)\mathcal{A}_{y,n} .
\end{aligned} \tag{2.8}$$

These coefficients are computed at a renormalisation scale fixed to the centre-of-mass energy, and are therefore just dimensionless numbers for each observable and each value of n.

The computation of the coefficients is carried out using the parton-level event generator program `EERAD3` [3, 50], which contains the relevant matrix elements with up to five external partons [51–54], combined using an infrared antenna subtraction method [55]. A recently discovered inconsistency in the treatment of large-angle soft radiation terms [6] in the original `EERAD3` implementation has been corrected. They account for an initially observed discrepancy between the `EERAD3` results and the logarithmic contributions (computed within SCET) to the thrust distribution to NNLO [56], which are now in full agreement.

In terms of the running coupling $\alpha_s(\mu^2)$, the NNLO expression for an event shape moment measured at centre-of-mass energy squared s becomes:

$$\begin{aligned}
\langle y^n \rangle(s, \mu^2) = &\left(\frac{\alpha_s(\mu)}{2\pi}\right)\bar{\mathcal{A}}_{y,n} + \left(\frac{\alpha_s(\mu)}{2\pi}\right)^2 \left(\bar{\mathcal{B}}_{y,n} + \bar{\mathcal{A}}_{y,n}\beta_0 \log\frac{\mu^2}{s}\right) \\
&+ \left(\frac{\alpha_s(\mu)}{2\pi}\right)^3 \left(\bar{\mathcal{C}}_{y,n} + 2\bar{\mathcal{B}}_{y,n}\beta_0 \log\frac{\mu^2}{s} + \bar{\mathcal{A}}_{y,n}\left(\beta_0^2 \log^2\frac{\mu^2}{s} + \beta_1 \log\frac{\mu^2}{s}\right)\right) \\
&+ \mathcal{O}(\alpha_s^4) .
\end{aligned} \tag{2.9}$$

3. NNLO contributions

The perturbative LO and NLO coefficients $\mathcal{A}_{y,n}$, $\mathcal{B}_{y,n}$ have been known for many years [57–60], and have been used extensively in the experimental studies of LEP data. Our major new results presented here are the perturbative NNLO coefficients $\mathcal{C}_{y,n}$. These coefficients receive contributions from six different colour factors:

$$N^2\,, \quad N^0\,, \quad 1/N^2\,, \quad N_F\,N\,, \quad N_F/N\,, \quad N_F^2\,.$$

We have computed these six different contributions separately.

The evaluation of the perturbative coefficients $\mathcal{A}_{y,n}$, $\mathcal{B}_{y,n}$ and $\mathcal{C}_{y,n}$ requires the numerical integration of the weighted perturbative event shape distributions down to the exact two-jet boundary $y = 0$. At this boundary, all event shape distributions diverge like $1/y$, and are further enhanced by large logarithmic corrections at NLO and NNLO. Since the integrand for the n-th moment is the distribution weighted by y^n, the moments themselves are finite. The first moment does however contain an integrable logarithmic singularity, and thus receives sizable contributions from the region $y \to 0$.

The numerical convergence of the perturbative coefficients computed by `EERAD3` deteriorates for $y \to 0$ for the following reason. The four-particle and five-particle phase spaces in `EERAD3` are generated with a lower cut-off δ_0 on all dimensionless invariants s_{ij}/s. This cut-off is required to avoid sampling kinematical regions where the numerical evaluation of the four-parton one-loop matrix element becomes unstable due to the presence of large inverse Gram determinants, and also to avoid regions where the antenna subtraction procedure induces cancellations over too many orders of magnitude for the remainder to be evaluated reliably. The independence of the results on δ_0 serves as a check for the proper implementation of the subtraction. In our calculation of the event shape distributions [1], we used $\delta_0 = 10^{-5}$ as a default, observing that this value allowed a reliable evaluation of all contributions while ensuring numerical stability and convergence. In approaching $y \to \delta_0$ from above, the unresolved invariants are no longer small compared to the resolved invariants, and the calculation is likely to miss parts of the finite remainder from the subtraction. For $y < \delta_0$, no reliable evaluation is possible. Consequently, we have to impose a lower cut y_0 on y when evaluating the perturbative coefficients. This cut is likely to affect especially the first moment. Due to the strong suppression of the $y \to 0$ region in the higher moments, this cut does not play a role for $n \geq 2$.

Therefore, in evaluating the perturbative coefficients, especially for the first moment, we carried out systematic studies to determine the values for the technical parameters δ_0 and y_0. It is observed that $y_0 = 10^{-5}$ is sufficient for all observables. In approaching this value, one observes already a reasonable convergence of all colour factor contributions to the first moments, and from studies with lower values of $y_0 < 10^{-5}$, we estimate the contribution from this region to each colour factor not to exceed five per cent of the total. The choice of δ_0 depends on the event shape variable under consideration. Already at NLO, one observes that $\delta_0 = y_0/10$ is sufficiently small for a reliable evaluation of the first moment of $(1 - T)$, ρ, C and Y_3, while B_W and B_T require much smaller δ_0. In the distribution of both broadenings, one observes that a cut δ_0 induces a modification of

the distributions up to $y \approx \sqrt{\delta_0}$, thereby rendering the numerical evaluation of the first moment of the broadenings much more challenging. This effect is illustrated in Figure 1 for the NLO-contribution to the B_W distribution, evaluated for different values of δ_0. For the NNLO contributions to the first moment of the broadenings, we chose $\delta_0 = 10^{-7}$, which is clearly a compromise between the accuracy of the evaluation and the numerical convergence. We have verified for both broadenings that for fixed $y_0 = 10^{-5}$, the numerical values of first moments do stabilize at $\delta_0 = 10^{-7}$, and we estimate that the individual colour factor contributions do not change by more than three per cent for lower δ_0. Full studies with much lower δ_0 were however not possible because of rapid deterioration of the numerical convergence. For these reasons, a systematic error of about 50% on the first moments of the broadenings should be taken into account.

In Tables 1 and 2, we list the individual colour factor contributions to the first five moments of the different event shape variables. Table 3 contains the total LO, NLO and NNLO coefficients. The moments given in Tables 1 to 3 have been calculated with $\delta_0 = 10^{-7}$ for B_W and B_T, where studies of other δ_0 values lead us to a systematic error estimate of 10% (except for the first moment, where the systematic error is estimated at 50%). For the other event shape variables, the default for the first moments is $\delta_0 = 10^{-6}$ with a systematic error of 6%, while the values for the higher moments have been calculated with $\delta_0 = 10^{-5}$ and studies of other δ_0 values result in a systematic error estimate of 3% for $(1-T)$, ρ, C and Y_3.

The behaviour in the different event shape variables is best seen by considering the ratios

$$K_{\mathrm{NLO}} = \frac{\bar{\mathcal{A}}_{y,n} + \bar{\mathcal{B}}_{y,n}\,\left(\frac{\alpha_s}{2\pi}\right)}{\bar{\mathcal{A}}_{y,n}} \tag{3.1}$$

and

$$K_{\mathrm{NNLO}} = \frac{\bar{\mathcal{A}}_{y,n} + \bar{\mathcal{B}}_{y,n}\,\left(\frac{\alpha_s}{2\pi}\right) + \bar{\mathcal{C}}_{y,n}\,\left(\frac{\alpha_s}{2\pi}\right)^2}{\bar{\mathcal{A}}_{y,n}}\,, \tag{3.2}$$

which we display for $\alpha_s = 0.124$ in Figures 2–4. Although substantially above the world average, it turned out that this value of α_s is the best-fit result [42] of fitting the pure NNLO predictions to event shape data from ALEPH. Consequently, we also employ this value in the event shape studies here. We observe that the perturbative corrections affect the different shape variables in a substantially different manner, which was already evident at NLO (see for example [13]). While the size of the corrections is largely independent of n for ρ, B_W and Y_3 (and roughly $\mathcal{K} \approx 1.3$ at NNLO for all three variables), it increases with n for $(1-T)$, C and B_T (amounting to $\mathcal{K} \approx 3$ for $n = 5$ for all three variables). This picture is consistent with the observations made on the perturbative stability of the distributions [1], where the former three displayed uniform and moderate NNLO corrections, resulting in a stabilization of the perturbative expansion, while the latter three suffered large corrections.

4. Numerical results and comparison to data

Moments of event shapes have been measured by various e^+e^- collider experiments at centre-of-mass energies ranging from 10 GeV to 206 GeV [61]. These data are particularly interesting in view of the determination of non-perturbative power corrections. Since the power correction contributions scale like inverse powers of the centre-of-mass energy Q, one needs a large range in energies to empirically disentangle their contribution from the perturbative contribution, which scales logarithmically with the energy.

However, even based on data covering about a factor twenty in energy range, missing higher order contributions may be misidentified as power corrections. The accuracy on the extraction of power correction contributions from data is therefore inherently linked to the precision of the perturbative prediction. We therefore expect the NNLO corrections computed here to lead to a considerable improvement of the power correction extraction from event shape moments.

In Figure 5, we computed the energy dependence of the first moments of all event shape variables for $\alpha_S(M_Z) = 0.124$ at LO, NLO and NNLO. The theory uncertainty at each order is estimated by varying the renormalization scale in the strong coupling constant in the range $Q/2 < \mu_R < 2\,Q$. The theory predictions are compared to data from JADE and OPAL [61]. It can be clearly seen that the inclusion of the NNLO corrections leads to a substantial reduction (by a factor two to three compared to NLO) of the theoretical uncertainty in all variables. The theory error bands at NLO and NNLO generally overlap (although the overlap is only marginal for $(1-T)$, C and B_T, which have the largest corrections, see above). We observe that the energy dependence of the first moment is well described by the purely perturbative NNLO QCD contribution for Y_3, while all other observables require the presence of additional non-perturbative contributions at low centre-of-mass energies. Comparing NLO and NNLO predictions, we observe that the NNLO contribution comes closer to the experimental data at low Q by about 30% for $1-T$ and C, while only little improvement over NLO is observed for the other observables. The low-Q discrepancy between data and NNLO theory is most pronounced in ρ, C and $(1-T)$. It is especially interesting to note that the required size of the power correction contribution is uncorrelated with size of the perturbative higher order corrections: both ρ and Y_3 receive only moderate NLO and NNLO corrections; to describe the low-energy data on the first moment of ρ, one must postulate substantial (larger than in any other observable) power corrections, while data on Y_3 are well described without power corrections.

The higher moments of the six standard event shapes are displayed in Figures 6 $(1-T)$, 7 (ρ), 8 (C), 9 (Y_3), 11 (B_T) and 10 (B_W). The predictions are compared to JADE and OPAL data [61]. The qualitative behaviour of the higher moments of the different shape variables is similar to what was observed for the first moments. For $(1-T)$, C and B_T, we again observe that the NLO and NNLO theory error bands merely overlap. Despite the increase in the size of the NNLO corrections to the higher moments, this situation does not deteriorate for higher n, mainly because of the equally large increase of the NLO corrections. This behaviour should however be taken as an indication of the poor perturbative convergence of these three observables. For all n, we observe a

substantial discrepancy between NNLO theory and experimental data at low-Q in ρ, C and $(1-T)$ and B_T, indicating large power corrections to these observables. The relative size of the discrepancy does not decrease with n, illustrating the relevance of power corrections throughout the full kinematical range of the event shape variable (and not only in the two-jet region). Data on the higher moments of B_W and Y_3 are well described by NNLO theory, leaving only little room for power correction contributions to these observables.

With the new NNLO corrections, the theory uncertainty is reduced to the few per cent level for the moments of all event shape observables. It should therefore now be possible to perform precise studies of power corrections on these data sets.

5. Conclusions and Outlook

In this paper, we have computed the NNLO corrections to moments of the six most commonly studied event shape variables: $(1-T)$, ρ, C, B_T, B_W and Y_3. Especially the first moment receives substantial contributions from kinematical configurations deep inside the two-jet region, well beyond the region probed by event shape distributions. Consequently, the evaluation of the first moment is technically demanding, in particular for the jet broadenings.

The NNLO corrections to the first moment are moderate for all event shapes, leading to a $\mathcal{K}$-factor of order unity (in the range 0.95 to 1.4 for the different shapes). For higher moments, we observed that the NNLO corrections to the moments of $(1-T)$, C and B_T increase with increasing moment number n, resulting in large NNLO $\mathcal{K}$-factors of up to 3. For B_W, ρ and Y_3, we observe that the corrections remain moderate towards higher n, indicating the better perturbative stability of these three variables.

The energy dependence of the event shape moments can be used for the empirical determination of power corrections due to non-perturbative effects. For these studies, a reliable description of the perturbative contributions is mandatory. We observe that the newly computed NNLO corrections lead to a substantial reduction of the theoretical uncertainty on these predictions. From a comparison with data from JADE and OPAL, we observe that the energy dependence of the moments of B_W and Y_3 can be largely described without any power corrections, while the other observables show clear indications for power-like contributions at low centre-of-mass energy.

In view of the newly computed NNLO perturbative corrections, it will be very interesting to revisit the existing non-perturbative power correction models. Given the considerably reduced uncertainty on the perturbative prediction, a more precise extraction of hadronization parameters can now be envisaged.

Acknowledgements

AG and TG would like to acknowledge the Aspen Center of Physics, where part of this work was carried out. GH would like to thank the ITP, University of Zürich for hospitality. EWNG gratefully acknowledges the support of the Wolfson Foundation and the Royal Society. This research was supported in part by the Swiss National Science Foundation (SNF)

under contracts PP0022-118864 and 200020-117602, by the UK Science and Technology Facilities Council and by the European Commission's Marie-Curie Research Training Network under contract MRTN-CT-2006-035505 "Tools and Precision Calculations for Physics Discoveries at Colliders".

References

[1] A. Gehrmann-De Ridder, T. Gehrmann, E. W. N. Glover and G. Heinrich, JHEP **0712** (2007) 094 [arXiv:0711.4711].

[2] A. Gehrmann-De Ridder, T. Gehrmann, E. W. N. Glover and G. Heinrich, Phys. Rev. Lett. **99** (2007) 132002 [arXiv:0707.1285].

[3] A. Gehrmann-De Ridder, T. Gehrmann, E. W. N. Glover and G. Heinrich, JHEP **0711** (2007) 058 [arXiv:0710.0346].

[4] S. Weinzierl, arXiv:0904.1077 [hep-ph].

[5] S. Weinzierl, arXiv:0904.1145 [hep-ph].

[6] S. Weinzierl, Phys. Rev. Lett. **101** (2008) 162001 [arXiv:0807.3241].

[7] S. Brandt, C. Peyrou, R. Sosnowski and A. Wroblewski, Phys. Lett. **12** (1964) 57; E. Farhi, Phys. Rev. Lett. **39** (1977) 1587.

[8] L. Clavelli and D. Wyler, Phys. Lett. B **103** (1981) 383.

[9] G. Parisi, Phys. Lett. B **74** (1978) 65;
J.F. Donoghue, F.E. Low and S.Y. Pi, Phys. Rev. D **20** (1979) 2759.

[10] P.E.L. Rakow and B.R. Webber, Nucl. Phys. B **191** (1981) 63;
S. Catani, G. Turnock and B. R. Webber, Phys. Lett. B **295** (1992) 269.

[11] S. Catani, Y.L. Dokshitzer, M. Olsson, G. Turnock and B.R. Webber, Phys. Lett. B **269** (1991) 432;
N. Brown and W.J. Stirling, Phys. Lett. B **252** (1990) 657; Z. Phys. C **53** (1992) 629;
W.J. Stirling *et al.*, Proceedings of the Durham Workshop, J. Phys. **G17** (1991) 1567;
S. Bethke, Z. Kunszt, D.E. Soper and W.J. Stirling, Nucl. Phys. B **370** (1992) 310 [Erratum-ibid. B **523** (1998) 681].

[12] P. A. Movilla Fernandez, O. Biebel, S. Bethke, S. Kluth and P. Pfeifenschneider [JADE Collaboration], Eur. Phys. J. C **1** (1998) 461 [hep-ex/9708034].

[13] G. Abbiendi *et al.* [OPAL Collaboration], Eur. Phys. J. C **40** (2005) 287 [hep-ex/0503051].

[14] P. Abreu *et al.* [DELPHI Collaboration], Phys. Lett. B **456** (1999) 322.

[15] P. Achard *et al.* [L3 Collaboration], Phys. Rept. **399** (2004) 71 [hep-ex/0406049].

[16] S. Kluth, P. A. Movilla Fernandez, S. Bethke, C. Pahl and P. Pfeifenschneider, Eur. Phys. J. C **21** (2001) 199 [hep-ex/0012044].

[17] A. V. Manohar and M. B. Wise, Phys. Lett. B **344** (1995) 407 [hep-ph/9406392].

[18] B. R. Webber, Phys. Lett. B **339** (1994) 148 [hep-ph/9408222].

[19] G. P. Korchemsky and G. Sterman, Nucl. Phys. B **437** (1995) 415 [hep-ph/9411211].

[20] Y. L. Dokshitzer and B. R. Webber, Phys. Lett. B **352** (1995) 451 [hep-ph/9504219].

[21] R. Akhoury and V. I. Zakharov, Phys. Lett. B **357** (1995) 646 [hep-ph/9504248].

[22] P. Nason and M. H. Seymour, Nucl. Phys. B **454** (1995) 291 [hep-ph/9506317].

[23] Y. L. Dokshitzer, G. Marchesini and B. R. Webber, Nucl. Phys. B **469** (1996) 93 [hep-ph/9512336].

[24] Y. L. Dokshitzer and B. R. Webber, Phys. Lett. B **404** (1997) 321 [hep-ph/9704298].

[25] M. Beneke, Phys. Rept. **317** (1999) 1 [hep-ph/9807443].

[26] Y. L. Dokshitzer, A. Lucenti, G. Marchesini and G. P. Salam, Nucl. Phys. B **511** (1998) 396 [Erratum-ibid. B **593** (2001) 729] [hep-ph/9707532].

[27] Y. L. Dokshitzer, A. Lucenti, G. Marchesini and G. P. Salam, JHEP **9805** (1998) 003 [hep-ph/9802381].

[28] G. P. Korchemsky and S. Tafat, JHEP **0010** (2000) 010 [hep-ph/0007005].

[29] A. V. Belitsky, G. P. Korchemsky and G. Sterman, Phys. Lett. B **515** (2001) 297 [hep-ph/0106308].

[30] E. Gardi and G. Grunberg, JHEP **9911** (1999) 016 [hep-ph/9908458].

[31] E. Gardi, JHEP **0004** (2000) 030 [hep-ph/0003179].

[32] E. Gardi and J. Rathsman, Nucl. Phys. B **609** (2001) 123 [hep-ph/0103217].

[33] E. Gardi and J. Rathsman, Nucl. Phys. B **638** (2002) 243 [hep-ph/0201019].

[34] J. M. Campbell, E. W. N. Glover and C. J. Maxwell, Phys. Rev. Lett. **81** (1998) 1568 [arXiv:hep-ph/9803254].

[35] M. Dasgupta and G. P. Salam, J. Phys. G **30** (2004) R143 [hep-ph/0312283].

[36] C. W. Bauer and I. W. Stewart, Phys. Lett. B **516** (2001) 134 [hep-ph/0107001].

[37] C. W. Bauer, D. Pirjol and I. W. Stewart, Phys. Rev. D **65** (2002) 054022 [hep-ph/0109045].

[38] C. W. Bauer, S. Fleming, D. Pirjol, I. Z. Rothstein and I. W. Stewart, Phys. Rev. D **66** (2002) 014017 [hep-ph/0202088].

[39] C. W. Bauer, S. P. Fleming, C. Lee and G. Sterman, Phys. Rev. D **78** (2008) 034027 [arXiv:0801.4569].

[40] P. A. Movilla Fernandez, S. Bethke, O. Biebel and S. Kluth, Eur. Phys. J. C **22** (2001) 1 [hep-ex/0105059].

[41] C. Pahl, S. Bethke, S. Kluth, J. Schieck and the JADE collaboration, arXiv:0810.2933.

[42] G. Dissertori, A. Gehrmann-De Ridder, T. Gehrmann, E. W. N. Glover, G. Heinrich and H. Stenzel, JHEP **0802** (2008) 040 [arXiv:0712.0327].

[43] S. Bethke, S. Kluth, C. Pahl and J. Schieck [JADE Collaboration], arXiv:0810.1389.

[44] T. Gehrmann, G. Luisoni and H. Stenzel, Phys. Lett. B **664** (2008) 265 [arXiv:0803.0695].

[45] S. Catani, L. Trentadue, G. Turnock and B.R. Webber, Nucl. Phys. B **407** (1993) 3.

[46] R. A. Davison and B. R. Webber, Eur. Phys. J. C **59** (2009) 13 [arXiv:0809.3326].

[47] K. G. Chetyrkin, A. L. Kataev and F. V. Tkachov, Phys. Lett. B **85** (1979) 277.

[48] W. Celmaster and R. J. Gonsalves, Phys. Rev. Lett. **44** (1980) 560.

[49] M. Dine and J. R. Sapirstein, Phys. Rev. Lett. **43** (1979) 668.

[50] A. Gehrmann-De Ridder, T. Gehrmann, E. W. N. Glover and G. Heinrich, Phys. Rev. Lett. **100** (2008) 172001 [arXiv:0802.0813].

[51] L.W. Garland, T. Gehrmann, E.W.N. Glover, A. Koukoutsakis and E. Remiddi, Nucl. Phys. B **627** (2002) 107 [hep-ph/0112081] and **642** (2002) 227 [hep-ph/0206067].

[52] S. Moch, P. Uwer and S. Weinzierl, Phys. Rev. D **66** (2002) 114001 [hep-ph/0207043].

[53] E.W.N. Glover and D.J. Miller, Phys. Lett. B **396** (1997) 257 [hep-ph/9609474];
Z. Bern, L.J. Dixon, D.A. Kosower and S. Weinzierl, Nucl. Phys. B **489** (1997) 3 [hep-ph/9610370];
J.M. Campbell, E.W.N. Glover and D.J. Miller, Phys. Lett. B **409** (1997) 503 [hep-ph/9706297];
Z. Bern, L.J. Dixon and D.A. Kosower, Nucl. Phys. B **513** (1998) 3 [hep-ph/9708239].

[54] K. Hagiwara and D. Zeppenfeld, Nucl. Phys. B **313** (1989) 560;
F.A. Berends, W.T. Giele and H. Kuijf, Nucl. Phys. B **321** (1989) 39;
N.K. Falck, D. Graudenz and G. Kramer, Nucl. Phys. B **328** (1989) 317.

[55] A. Gehrmann-De Ridder, T. Gehrmann and E.W.N. Glover, JHEP **0509** (2005) 056 [hep-ph/0505111]; Nucl. Phys. B **691** (2004) 195 [hep-ph/0403057]; Phys. Lett. B **612** (2005) 36 [hep-ph/0501291]; **612** (2005) 49 [hep-ph/0502110].

[56] T. Becher and M.D. Schwartz, JHEP **0807** (2008) 034 [arXiv:0803.0342].

[57] R.K. Ellis, D.A. Ross and A.E. Terrano, Nucl. Phys. B **178** (1981) 421.

[58] Z. Kunszt, Phys. Lett. B **99** (1981) 429;
J.A.M. Vermaseren, K.J.F. Gaemers and S.J. Oldham, Nucl. Phys. B **187** (1981) 301;
K. Fabricius, I. Schmitt, G. Kramer and G. Schierholz, Z. Phys. C **11** (1981) 315.

[59] Z. Kunszt and P. Nason, in *Z Physics at LEP 1*, CERN Yellow Report 89-08, Vol. 1, p. 373.

[60] W.T. Giele and E.W.N. Glover, Phys. Rev. D **46** (1992) 1980;
S. Catani and M.H. Seymour, Nucl. Phys. B **485** (1997) 291; **510** (1997) 503(E) [hep-ph/9605323].

[61] C. J. Pahl, *Ph.D. thesis*, TU Munich 2007.

		$\langle(1-T)^n\rangle$	$\langle\rho^n\rangle$	$\langle C^n\rangle$	$\langle B_W^n\rangle$	$\langle B_T^n\rangle$	$\langle Y_3^n\rangle$
N^2	$n=1$	2301 ± 11	993 ± 12	8816 ± 37	348 ± 34	3007 ± 59	470 ± 5
	2	337.1 ± 0.6	120.5 ± 0.6	4413 ± 5	174 ± 1	745 ± 1	45.6 ± 0.3
	3	63.2 ± 0.2	15.7 ± 0.1	2381 ± 2	23.2 ± 0.2	145.6 ± 0.2	6.64 ± 0.07
	4	13.94 ± 0.02	2.42 ± 0.03	1471 ± 1	3.20 ± 0.03	32.13 ± 0.03	1.20 ± 0.01
	5	3.490 ± 0.005	0.438 ± 0.006	984 ± 2	0.456 ± 0.005	7.86 ± 0.01	0.249 ± 0.002
N^0	$n=1$	34.68 ± 0.12	85.6 ± 0.2	285.4 ± 0.4	4.0 ± 4.4	383 ± 2	14.38 ± 0.06
	2	-19.62 ± 0.01	-2.10 ± 0.01	-220.1 ± 0.2	7.66 ± 0.02	-21.64 ± 0.03	-1.181 ± 0.005
	3	-4.630 ± 0.002	-0.564 ± 0.003	-165.13 ± 0.06	-0.028 ± 0.002	-8.656 ± 0.005	-0.243 ± 0.002
	4	-1.1240 ± 0.0006	-0.0973 ± 0.0009	-113.92 ± 0.03	-0.0474 ± 0.0007	-2.285 ± 0.002	-0.0494 ± 0.0005
	5	-0.2938 ± 0.0001	-0.0163 ± 0.0003	-80.72 ± 0.03	-0.2938 ± 0.0001	-0.6025 ± 0.0005	-0.0102 ± 0.0001
$1/N^2$	$n=1$	0.202 ± 0.008	7.51 ± 0.03	3.31 ± 0.03	85.6 ± 0.2	16.17 ± 0.05	0.5788 ± 0.0041
	2	-0.2270 ± 0.0008	-0.0799 ± 0.0009	-4.900 ± 0.007	0.232 ± 0.001	-2.620 ± 0.004	-0.0205 ± 0.0007
	3	-0.0010 ± 0.0002	-0.0133 ± 0.0003	-0.931 ± 0.006	-0.0089 ± 0.0002	-0.3140 ± 0.0006	-0.00432 ± 0.0001
	4	0.00458 ± 0.00004	-0.00257 ± 0.00006	0.044 ± 0.004	-0.00196 ± 0.00003	-0.0467 ± 0.0001	-0.00077 ± 0.00004
	5	0.00197 ± 0.00001	-0.00065 ± 0.00002	0.308 ± 0.003	-0.00036 ± 0.00001	-0.00790 ± 0.00003	-0.00019 ± 0.00001

Table 1: Individual colour factor contributions to event shape moments at NNLO: N^2, N^0, $1/N^2$. The given errors are the statistical errors from the numerical integration. Systematic errors originating from technical cut parameters (see text) are not shown in the table.

		$\langle(1-T)^n\rangle$	$\langle\rho^n\rangle$	$\langle C^n\rangle$	$\langle B_W^n\rangle$	$\langle B_T^n\rangle$	$\langle Y_3^n\rangle$
$N_F\,N$	$n=1$	-1716 ± 18	-1085 ± 15	-6930 ± 80	-664 ± 33	-3279 ± 41	-451 ± 8
	2	-164 ± 1	-95.8 ± 0.9	-2244 ± 11	-172 ± 2	-434 ± 2	-36.7 ± 0.5
	3	-26.1 ± 0.2	-12.8 ± 0.2	-1034 ± 6	-21.6 ± 0.2	-70.6 ± 0.3	-5.42 ± 0.08
	4	-5.23 ± 0.04	-2.30 ± 0.04	-572 ± 4	-3.21 ± 0.04	-14.06 ± 0.06	-1.05 ± 0.02
	5	-1.202 ± 0.008	-0.47 ± 0.01	-351 ± 3	-0.56 ± 0.01	-3.23 ± 0.02	-0.218 ± 0.004
N_F/N	$n=1$	-6.67 ± 0.01	-67.92 ± 0.11	-85.48 ± 0.07	-465.2 ± 0.3	-182.6 ± 0.2	-6.33 ± 0.02
	2	7.74 ± 0.02	1.39 ± 0.02	102.9 ± 0.1	-3.16 ± 0.02	23.79 ± 0.03	0.642 ± 0.007
	3	1.478 ± 0.004	0.312 ± 0.003	59.29 ± 0.09	0.133 ± 0.003	4.903 ± 0.008	0.123 ± 0.001
	4	0.3179 ± 0.0005	0.0596 ± 0.0006	36.22 ± 0.05	0.0398 ± 0.0004	1.075 ± 0.002	0.0241 ± 0.0004
	5	0.0763 ± 0.0003	0.0129 ± 0.0002	23.49 ± 0.03	0.0072 ± 0.0001	0.2565 ± 0.0005	0.0052 ± 0.0002
N_F^2	$n=1$	253.9 ± 0.2	271.32 ± 0.19	1123.5 ± 0.5	738.3 ± 0.3	710.4 ± 0.2	83.24 ± 0.05
	2	12.14 ± 0.04	15.00 ± 0.04	173.2 ± 0.4	33.64 ± 0.07	27.79 ± 0.05	5.50 ± 0.02
	3	1.388 ± 0.007	2.001 ± 0.008	55.8 ± 0.2	3.829 ± 0.007	2.42 ± 0.01	0.792 ± 0.003
	4	0.213 ± 0.002	0.364 ± 0.001	22.2 ± 0.1	0.609 ± 0.002	0.240 ± 0.002	0.1479 ± 0.0008
	5	0.0368 ± 0.0004	0.0760 ± 0.0004	9.15 ± 0.07	0.1129 ± 0.0004	0.0111 ± 0.0005	0.0320 ± 0.0003

Table 2: Individual colour factor contributions to event shape moments at NNLO: $N_F\,N$, N_F/N, N_F^2. The given errors are the statistical errors from the numerical integration. Systematic errors originating from technical cut parameters (see text) are not shown in the table.

		$\langle(1-T)^n\rangle$	$\langle\rho^n\rangle$	$\langle C^n\rangle$	$\langle B_W^n\rangle$	$\langle B_T^n\rangle$	$\langle Y_3^n\rangle$
$\mathcal{A}$	$n=1$	2.1035	2.1035	8.6379	4.0674	4.0674	0.8942
	2	0.1902	0.1902	2.4317	0.3369	0.3369	0.08141
	3	0.02988	0.02988	1.0792	0.04755	0.04755	0.01285
	4	0.005858	0.005858	0.5685	0.008311	0.008311	0.002523
	5	0.001295	0.001295	0.3272	0.001630	0.001630	0.0005570
$\mathcal{B}$	$n=1$	44.999 ± 0.002	23.342 ± 0.002	172.778 ± 0.007	-9.888 ± 0.006	63.976 ± 0.006	12.689 ± 0.135
	2	6.2595 ± 0.0004	3.0899 ± 0.0008	81.184 ± 0.005	4.5354 ± 0.0005	14.719 ± 0.001	1.2929 ± 0.0001
	3	1.1284 ± 0.0001	0.4576 ± 0.0002	42.771 ± 0.003	0.6672 ± 0.0001	2.7646 ± 0.0003	0.19901 ± 0.00005
	4	0.24637 ± 0.00003	0.08363 ± 0.00003	25.816 ± 0.002	0.10688 ± 0.00002	0.60690 ± 0.00006	0.03777 ± 0.00001
	5	0.06009 ± 0.00001	0.01759 ± 0.00001	16.873 ± 0.001	0.01865 ± 0.00001	0.14713 ± 0.00002	0.00804 ± 0.00001
$\mathcal{C}$	$n=1$	867.60 ± 21.19	204.55 ± 19.79	3212.2 ± 88.7	46.2 ± 47.8	655.5 ± 72.0	110.6 ± 9.3
	2	172.80 ± 1.22	38.93 ± 1.12	2220.9 ± 12.0	40.7 ± 1.9	337.8 ± 2.5	13.84 ± 0.62
	3	35.38 ± 0.26	4.626 ± 0.196	1296.6 ± 6.7	5.61 ± 0.26	73.34 ± 0.36	1.892 ± 0.107
	4	8.13 ± 0.04	0.445 ± 0.051	843.1 ± 3.9	0.591 ± 0.051	17.06 ± 0.07	0.274 ± 0.027
	5	2.109 ± 0.009	0.0367 ± 0.0121	585.0 ± 3.2	-0.273 ± 0.011	4.29 ± 0.02	0.0585 ± 0.005

Table 3: Contributions to event shape moments at LO, NLO, NNLO.

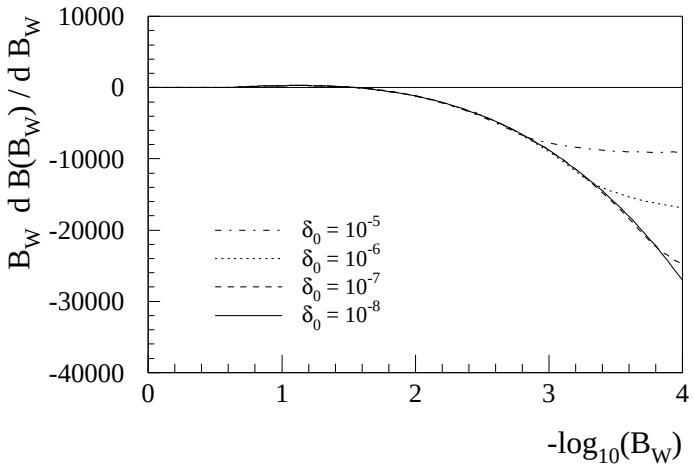

Figure 1: The NLO contribution to the wide jet broadening distribution $B_W\, dB(B_W)/dB_W$ evaluated for different technical cut-offs δ_0 on all phase space variables.

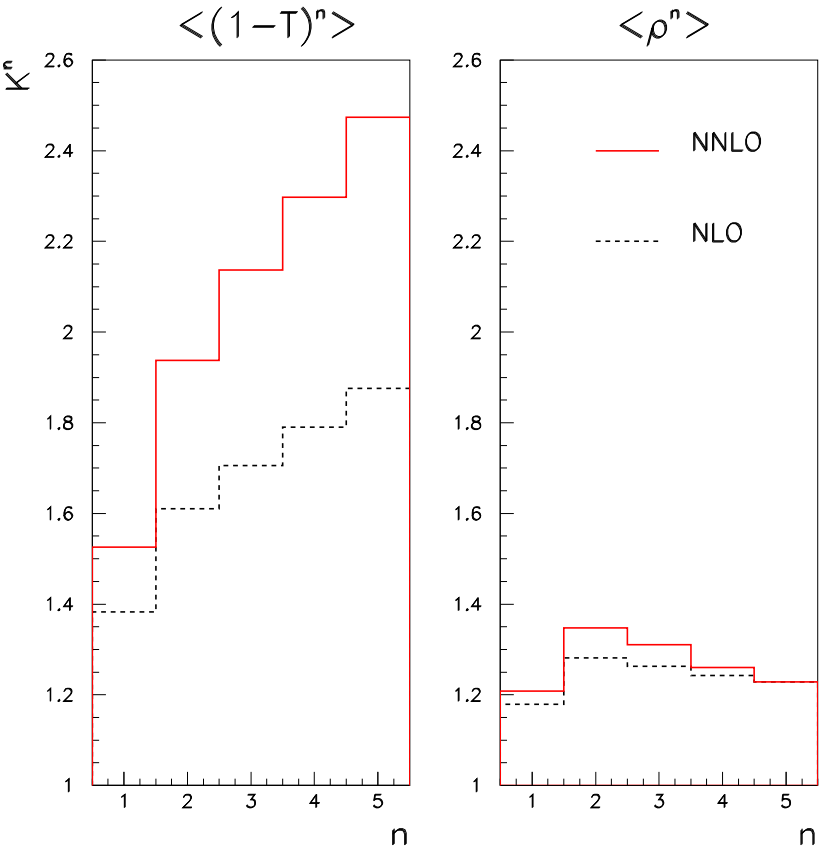

Figure 2: The ratios $K_{\rm NNLO}$ ($K_{\rm NLO}$) of the NNLO (NLO) corrections relative to LO for the first five moments of the thrust and heavy mass distributions evaluated at $\mu = Q$ with $\alpha_s = 0.124$.

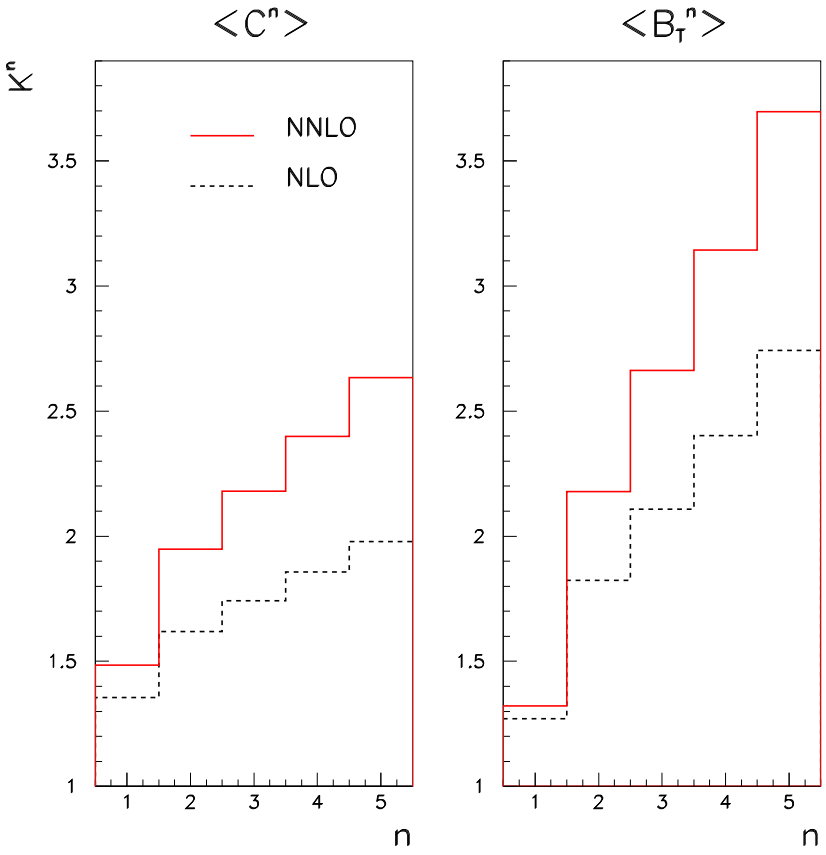

Figure 3: The ratios $K_{\rm NNLO}$ ($K_{\rm NLO}$) of the NNLO (NLO) corrections relative to LO for the first five moments of the C-parameter and total jet broadening distributions evaluated at $\mu = Q$ with $\alpha_s = 0.124$.

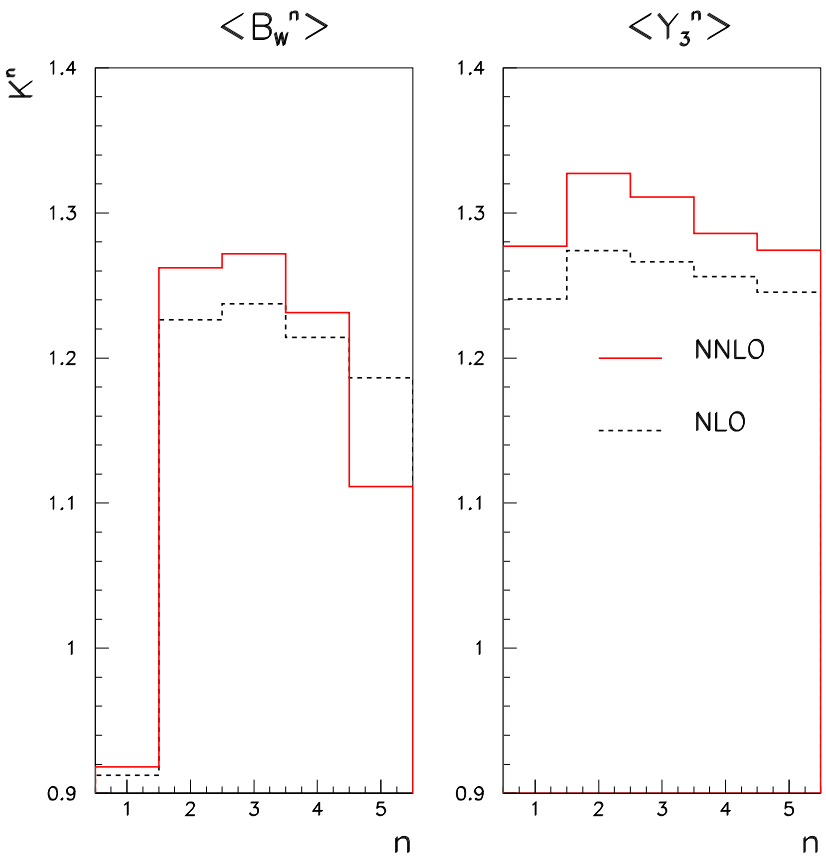

Figure 4: The ratios $K_{\rm NNLO}$ ($K_{\rm NLO}$) of the NNLO (NLO) corrections relative to LO for the first five moments of the wide jet broadening and Y_3 distributions evaluated at $\mu = Q$ with $\alpha_s = 0.124$.

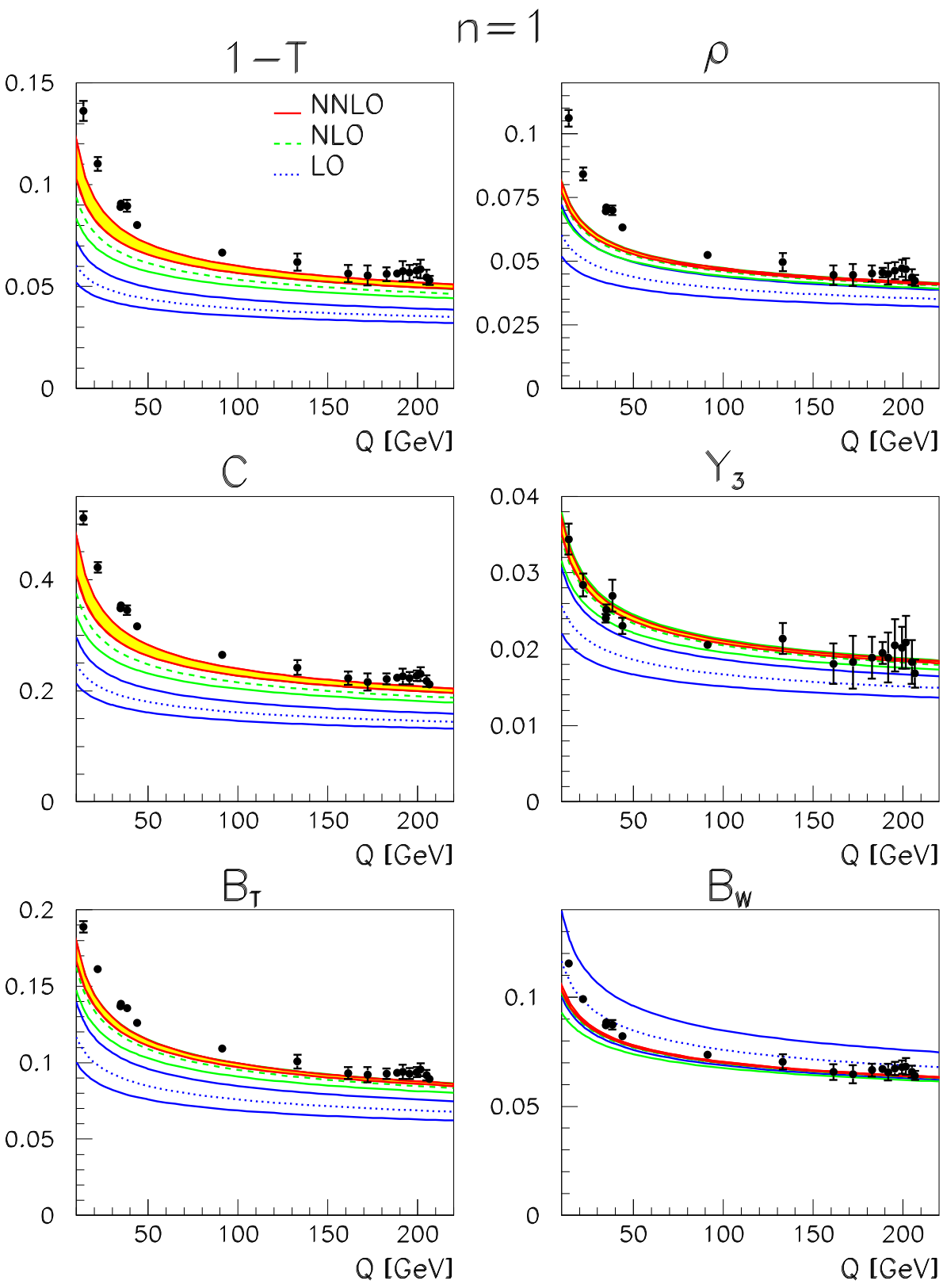

Figure 5: First moments of six event shape variables. The bands show the scale variations obtained by using $\mu = 2Q$ and $\mu = Q/2$. The data are from the JADE and OPAL experiments, taken from [61].

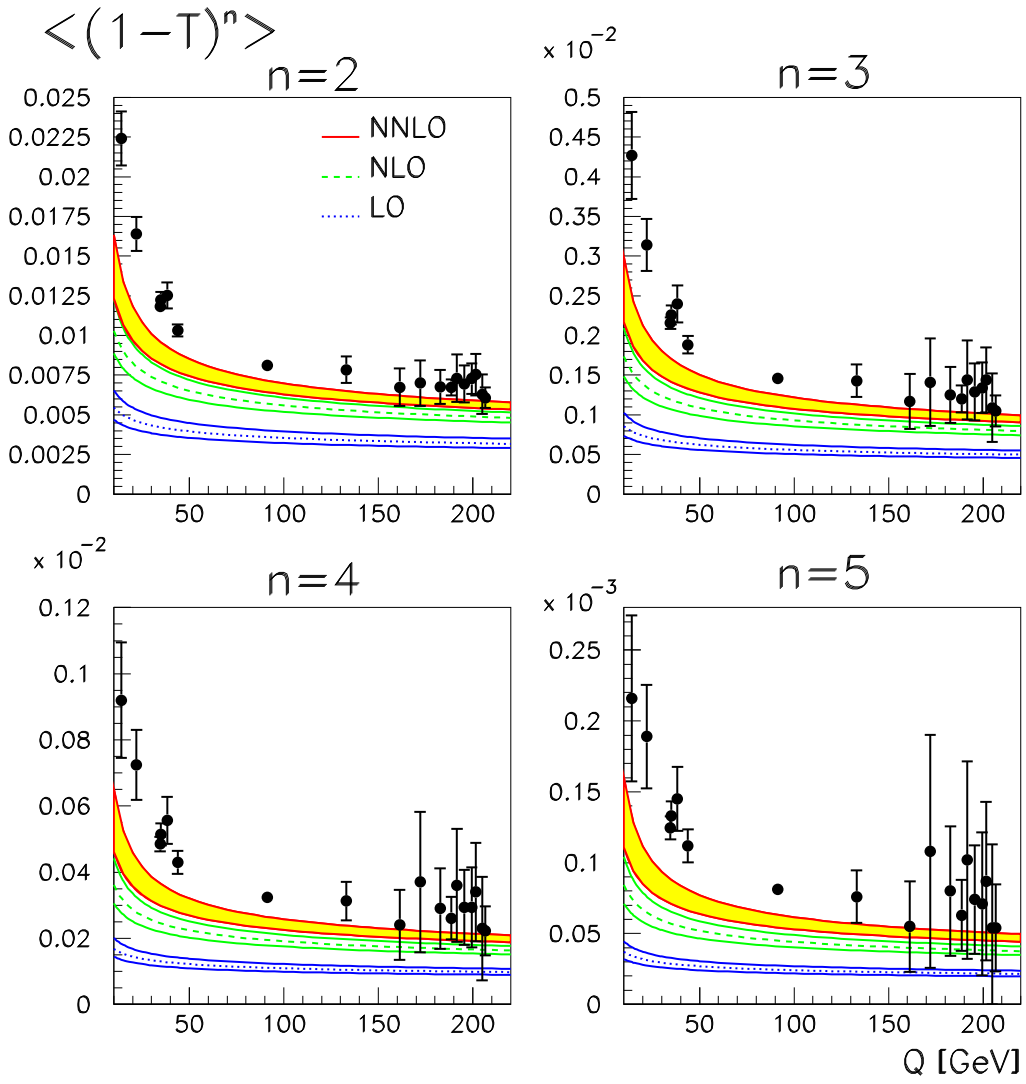

Figure 6: Perturbative corrections to the higher moments of $1 - T$. The bands show the scale variations obtained by using $\mu = 2Q$ and $\mu = Q/2$. The data are taken from [61].

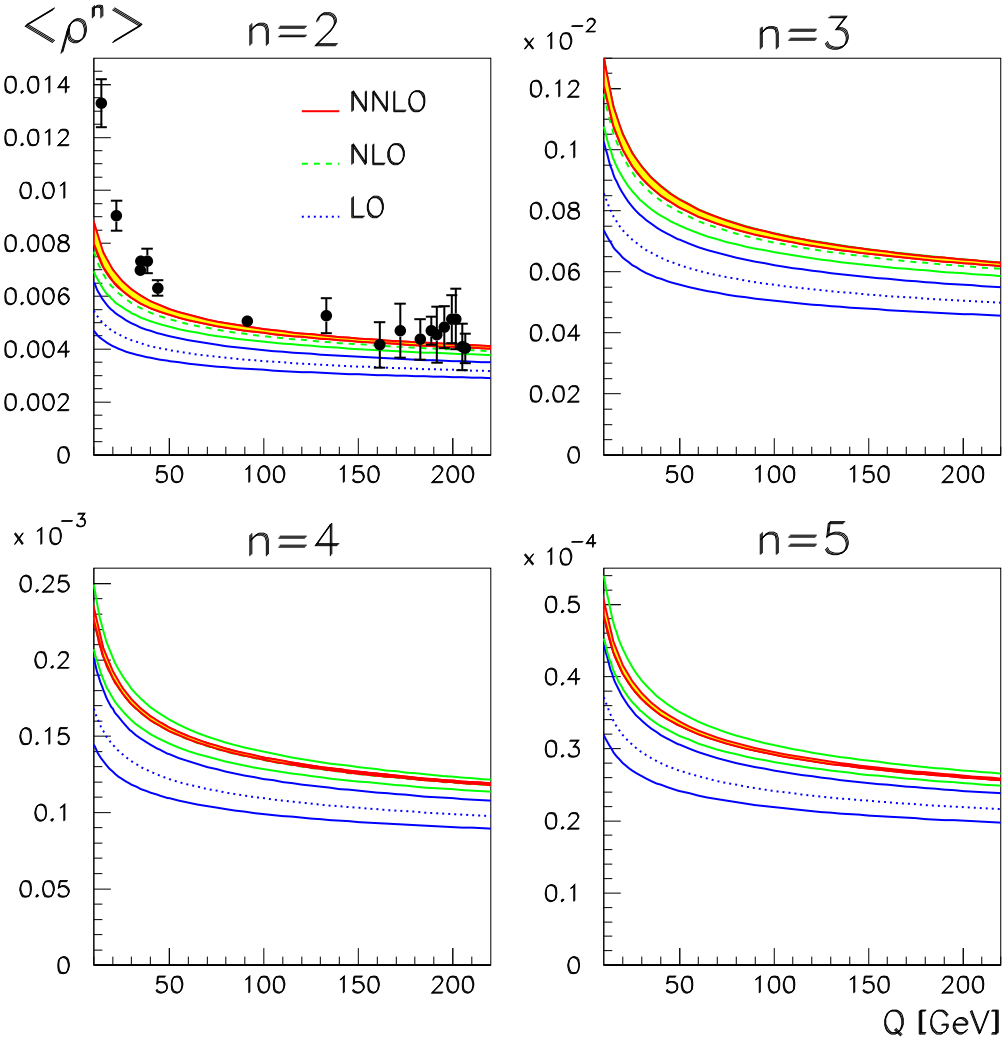

Figure 7: Perturbative corrections to the higher moments of the normalised heavy jet mass ρ. The bands show the scale variations obtained by using $\mu = 2Q$ and $\mu = Q/2$. The data are taken from [61], which only contains data for the moments of $M_H = \sqrt{\rho}$, such that no data are shown for $n = 3, 4, 5$.

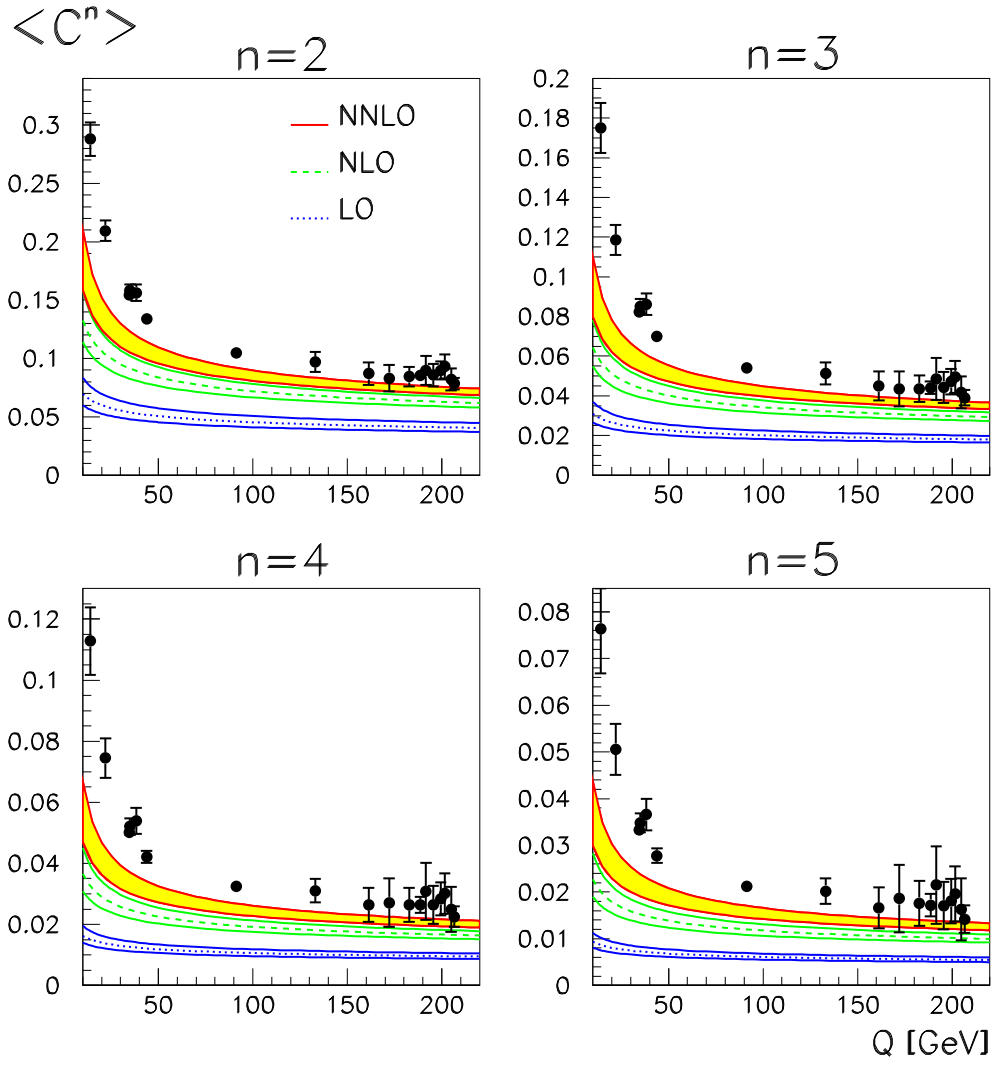

Figure 8: Perturbative corrections to the higher moments of the C-parameter. The bands show the scale variations obtained by using $\mu = 2Q$ and $\mu = Q/2$. The data are taken from [61].

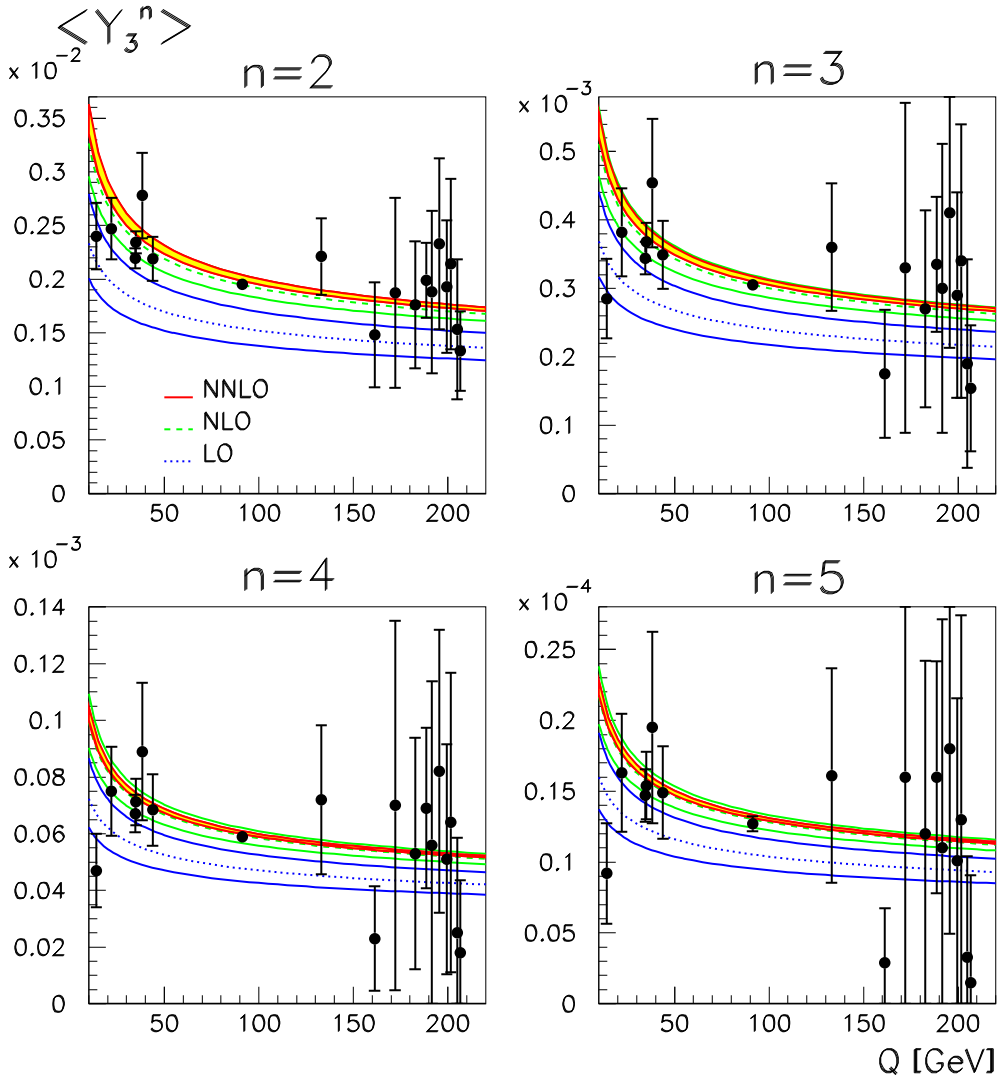

Figure 9: Perturbative corrections to the higher moments of the 2-jet to 3-jet transition parameter Y_3. The bands show the scale variations obtained by using $\mu = 2Q$ and $\mu = Q/2$. The data are taken from [61].

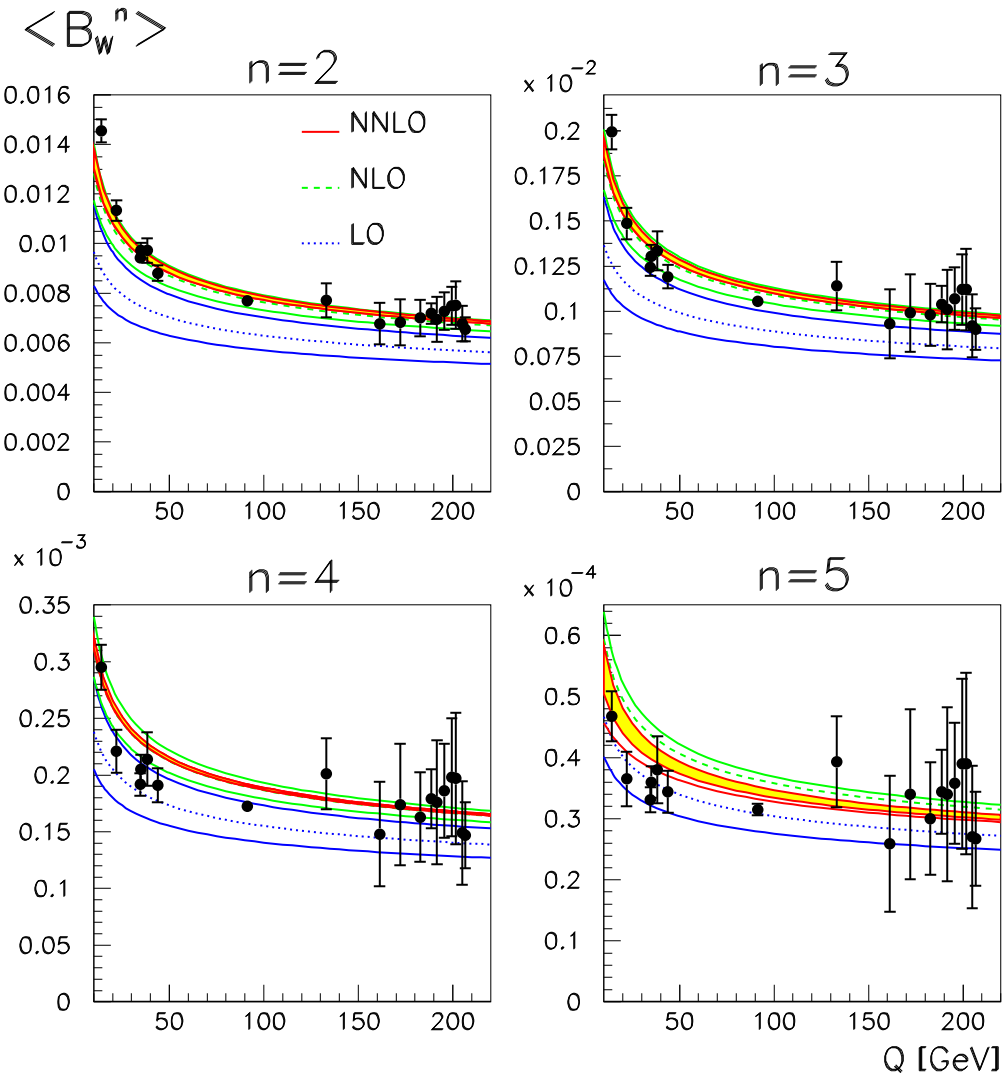

Figure 10: Perturbative corrections to the higher moments of the wide jet broadening B_W. The bands show the scale variations obtained by using $\mu = 2Q$ and $\mu = Q/2$. The data are taken from [61].

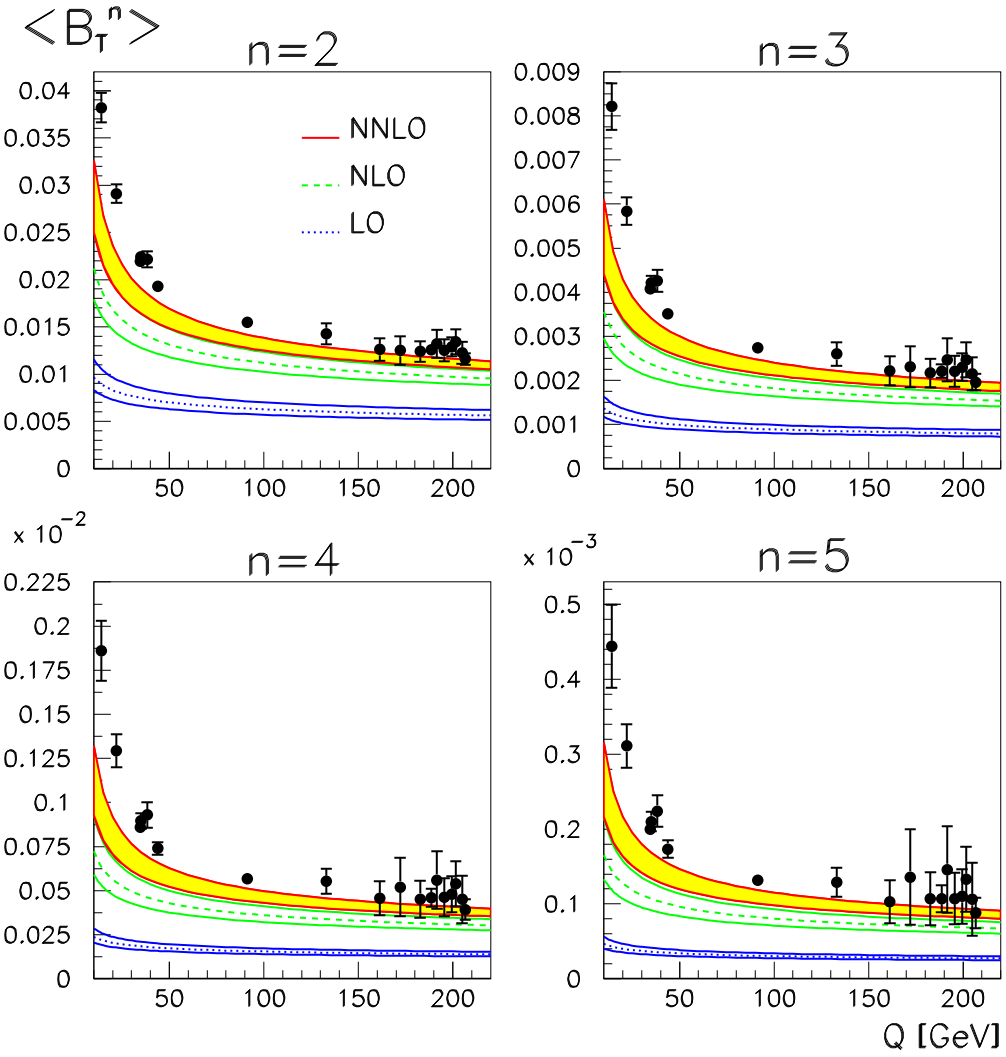

Figure 11: Perturbative corrections to the higher moments of the total jet broadening B_T. The bands show the scale variations obtained by using $\mu = 2Q$ and $\mu = Q/2$. The data are taken from [61].